2016 International Conference on Intelligent Manufacturing and Materials (ICIMM 2016)
ISBN: 978-1-60595-363-2

A Novel Method for Feature Extraction and Automatic Recognition of Tire Defects Using Independent Component Analysis

Xue Hong Cui, Yun Liu, Chuan Xu Wang and Hui Li

ABSTRACT

In order to extract the features of tire defects in X-ray images, Linear transformation is often performed on the images. However, Gabor and wavelet transformation are predefined and unchangeable, and their basic functions can't be adapted to the characteristics of defect images. So we propose a new approach using Independent Component Analysis (ICA) and Topographic Independent Component Analysis (TICA) reconstruction algorithm to extract the features of tire defects and apply automatic recognition of tire defects. First, the basis functions and filters which adapt to the characteristics of defect images are estimated adaptively using ICA and TICA from the tire defect library. Then, the tire defect images are filtered to extract features. Finally, the samples are classified by a nonlinear support vector machine (SVM). Experimental results show that the proposed algorithm has very high recognition rates for shape defects, texture defects and other defects. Its total recognition rate can be as high as 95.76%.

INTRODUCTION

Automated industrial defect inspection system is installed and used widely in factories to improve product quality and accelerate production. Currently domestic

XueHong Cui, Yun Liu, ChuanXu Wang, Hui Li School of Information Science and Technology, Qingdao University of Science and Technology, Qingdao, Shandong, China

and foreign scholars mainly have extracted geometrical features, texture features, gray features, invariant moment characteristics of defect images to identify defect images, and the recognition rate is only about 80% in the spatial domain[1]. Because some image characteristics are not obvious in the spatial domain, nevertheless, it becomes obvious in the transform domain [2-9]. some scholars transform defect images to the spectral domain to extract features, such as wavelet transforms, Fourier transforms, or Gabor transforms. However, since these transformations are predefined and unchangeable [8,9], the basic functions of these transforms are not related to the characteristics of defect images. So we propose a new approach using ICA and TICA reconstruction algorithm to extract the features of tire defects and apply automatic recognition of tire defects.

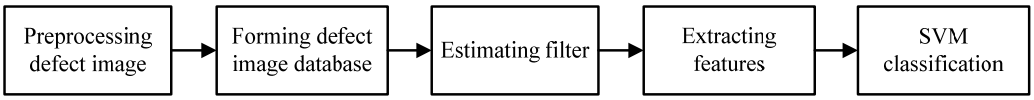

Figure 1. The flowchart of algorithm.

This paper is organized as follows. In section 2, we propose a new feature extraction algorithm by using ICA and TICA models. Section 3 details the estimation of filter bank and the basis function using our algorithm and discusses their advantages and points out the disadvantages of predefined basis function. In section 4, we present feature extraction of defect images using the presented filter bank method. Section 5 presents the experimental results and the performance evaluation on the tire defect datasets that we have built. Finally, some conclusions are given in section 6.

ICA AND TICA MODELS

ICA Model

Let us denote the observed data vector by $x=[x_1,x_2,\ldots,x_n]^{\mathrm{T}}$ which is modeled as a linear combination of the source signals $s=[s_1,s_2,\ldots,s_n]^{\mathrm{T}}$, And $A=[a_1,a_2,\ldots,a_n]^{\mathrm{T}}$ is the mixing matrix. The basic ICA model is shown as follows：

$$x = As = \sum_{i=1}^{n} a_i s_i \tag{1}$$

In case of an unknown s,A, ICA aims to estimate the unmixing matrix $W=[w_1,w_2,\cdots w_n]^T$ which is only based on the observed data x, and yields a

vector $y = Wx$, which results in the component of y being as statistically independent as possible, and y is an estimate of source signal s. When ICA is used in the image data, the basis function a_i are the columns vector of the matrix A, the filter w_i is the rows vector of matrix W.

There are several iterative algorithms to ICA. This paper have used Hyvärinens Fast ICA algorithm [12]. Usually a PCA preprocessing step is included for whitening of the data.

TICA Model

Hyvarinen proposed TICA algorithm[11] which relax the assumption of the independence of source signals s_i. s_i is given as follows:

$$s_i = \phi(\sum_{k=1}^{k} h(i,k)u_k)z_i \tag{2}$$

Here, $h(i,k)$ is a neighborhood function, neighborhood can be defined as one-dimensional or two-dimensional, $\phi(x) = x^{-1/2}$, u_i and z_i are all mutually independent, u_i is an independent random variables, z_i is the whitened dimension-reduced data of observation data x . We use the algorithm of paper [11] to solve TICA .

ESTIMATING BASIS FUNCTION AND FILTER

ICA is applied to digital images. the image $I(x,y)$ can be represented as a linear sum of its basis functions $a_i(x,y)$.

$$I(x,y) = \sum_{i=1}^{n} a_i(x,y)s_i \tag{3}$$

Here, s_i is a weighted factor. Once the basis functions a_i has been estimated, we can compute its corresponding filter $w_i^T(x,y)$, and then the independent component s_i can be computed by

$$s_i = \sum_{x,y} w_i(x,y)I(x,y) \tag{4}$$

In this paper, we learn the tire defects based on the tire X-ray images. For estimating the basis functions, unsupervised learning is carried out on a large number of defect samples. We represent an image as a column vector. Then all

defect samples form the corresponding column vector matrix as the observation data of ICA, TICA model. And then the mixing matrix A and demixing matrix W are estimated from the observation data. Then the column vector of the A is the basis functions a_i and the row vector of W is the filters wiT. In order to research the more intuitive, the basic function can be expressed as a two-dimensional image. Figure 2-3 are an example of ICA and TICA basis functions respectively for tire defect images. Here is the result of the 60 dimension after dimension reduction.

Figure 3 can be seen that this basis vectors are similar to Figure 2 estimated by ICA [10]. In addition, TICA[11] bases have a clear topographic organization (as for the topography we chose a 2-D torus lattice[12]). But the phases of nearby basis vectors are very different, giving each neighborhood properties similar to those of complex cells. The experiment results also show that this ordered representation is better than the ICA basis which is an unordered representation on the recognition performance of tire defects.

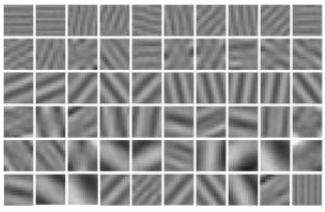

Figure 2. ICA basis functions.

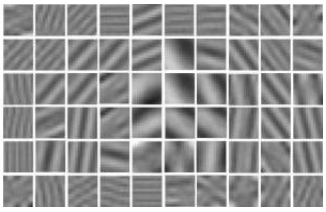

Figure 3. TICA basis functions.

FEATURE EXTRACTION OF DEFECT IMAGES

This section extract the linear and nonlinear feature for images. The linear feature is extracted as follows:

$$s_i = \langle w_i, I \rangle \tag{5}$$

The TICA filter has the same properties as the ICA filter. And the TICA filters also can be used to extract the linear features of defect images by using the formula (5). In addition to extracting the linear feature, TICA filter can extract the nonlinear feature by using the formula (6).

$$e_i = \left(\sum_{j=1}^{k} h(i,j)(w_j^{\mathrm{T}} I)^2 \right)^{\frac{1}{2}} \tag{6}$$

Where, $h(i,j)$ is the neighborhood function, w_j^T is the TICA filter. Compared with the responses s_i of the underlying linear filters, the responses e_i of topographic neighborhoods was computed as the local energy which the local energies are computed by first taking the squares of the outputs of linear filters, and then summing these squares inside a topographic neighborhood, then square root may be taken for normalization. The linear and nonlinear features of defect image were extracted respectively by ICA and TICA filter which are shown in Figure 4-5.

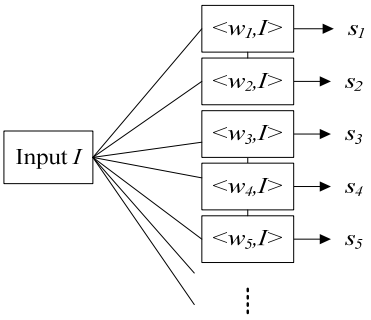

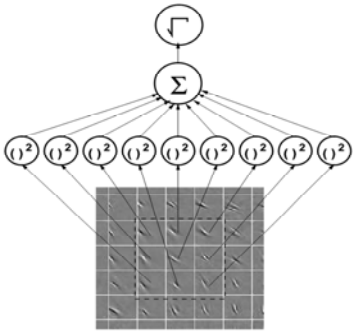

Figure 4. Extracting linear features.

Figure 5. Extracting nonlinear features.

Our proposed scheme is summarized as follows.

Step1. Collecting sufficient number of defect images. The number of each type of defect samples is proportional to the number of times it appears.

Step2. Estimating filter. Estimate the demixing matrix W using ICA and TICA respectively and the row vector of W is the estimated filters w_i^T.

Step3.Extracting features. Three kinds of features are extracted for the training samples or the test sample. The linear features s_i were extracted respectively by ICA and TICA filter using the formula (5),and the extracted features are called respectively the ICA linear feature (feature 1) and the TICA linear feature (feature 2). The nonlinear features e_i were extracted by the TICA filter using the formula(6),and the nonlinear features e_i merge with feature 2 to form feature 3.

Step4.The sample features are trained and identified by support vector machine.

The filter can be estimated off-line. The computation complexity of this method is low for the O(MN), where M*N is the number of pixels of defect image. It is independent of each other to extracted each linear feature s_i or nonlinear feature e_i. Therefore, a parallel structure to implement this algorithm can significantly reduce execution time.

EXPERIMENTAL RESULTS AND ANALYSIS

This section evaluates our method in the tire defect datasets built. It was performed on Intel Core 2 Quad core processor Q9400 2.66GHz with 4 GB RAM and was programmed by MATLAB R2009b.

Construction of Defect Database

In order to verify the effectiveness of this method for tire defect identification, we collected 8 types of the most common defects, such as inclusion, beam splitting, etc, there are 1085 images in total from a domestic tire production line defect detection system. The number of each type of defect images is proportional to the number of times it appears, and the defect images are the smallest rectangular image that may contain the defect. Due to the uncertainty of defects in production, the size, length and width of the defect images are very different, basically distributed between 112 ×128 and 392 × 286 pixels. In order to unify the size of defect images and reduce the computational complexity, we will zoom each image to 50 x 50 pixels using bilinear interpolation, and use these images to construct a defect library. In this defect library, the 600 images are used to estimate the ICA and TICA filters. During identification, 300 samples were randomly selected from the remaining 485 images in defect library as the test samples. The number of each type of defect samples is selected based on the original proportion. Such a sample selection is repeated for 5 times and the final recognition rate is the average of these 5 recognition rates.

Determine the Number of Filters

In order to determine the optimal number of filters to achieve the highest recognition rate, different numbers of filters are estimated with the proposed method. And the recognition rate of test samples was calculated separately in the range of [1,253] which is the number of filters estimated. In Figure 6, it can be seen that fewer filters can achieve a high recognition rate. When the number of the ICA filter used to extract the linear feature of samples is 19, the recognition rate can achieve the highest. when the number of the TICA filter which is used to extract the linear feature of samples is 12, the recognition rate can achieve the highest. When the number of the TICA filter which is used to extract the linear feature and the nonlinear feature of samples is 48, the recognition rate can achieve the highest. Accordingly, we respectively use 19, 12 and 48 corresponding filters to extract the above 3 kinds of feature for recognition.

Experimental Results and Analysis

First, the features of the training samples are extracted and are used to train SVM classifier, and the RBF is chosen as the kernel function of SVM, then the test sample was recognized by SVM classifier. We analyze the experimental results from two aspects. We first compare the overall recognition rates of 3 different features. As shown in Figure 6, when the number of filters is optimal, the recognition rates of the three kinds of feature was 93.85%, 94.55% and 95.52%, respectively. Conclusions are as follows:

The proposed method is effective for tire defect identification. We compare the recognition rates by using different texture feature extraction algorithms that are in literature [1] and invariant moments[2] and wavelet Transform Algorithm[3] and Gabor Filter[4], their recognition rates are respectively 84.06%, 86.01%, 91.05%, 93.43%. It can be seen that the recognition rate of this method is higher than that of other methods. Compared with the ICA linear feature, TICA linear feature is better in recognition, and the number of filters used by the former is larger than that of the latter, namely, TICA algorithm can shorten the recognition time. This is because the basis vectors based on TICA have the topological organization, provide an ordered representation for data, while the basis vectors based on ICA are in disorder. So we can use the relatively smaller optimal filters (here is 12) to extract TICA linear features to identify, and the recognition rate is higher.

Through the integration of features (Integrating the linear features and nonlinear features based on TICA), the recognition rate is improved, but the optimal number of filters is relatively large (here is 48). This is because the integrated features contain more information and excellent properties (phase and translation invariance), and these characteristics require a higher dimension to show, and bring obvious advantages to the defect identification. So the optimal number of filters is increased when this feature is extracted, and the recognition rate is the highest among the 3 features.

As can be seen from the TABLE 1. The recognition rate of 00 belt dispersion line defects is only 80%, which is because the number of training samples is small. In the experiment, we found that if more 00 belt dispersion line defect images were added to the training, the training and test samples increases to 4 times, the recognition rate is up to 96.02%. The recognition rate of split belts defect and belts open root defect is relatively low. By observing the sample images which have been classified by mistakes, we found that the features of split belts defect images and belts open root defect images is very similar, so lead to the wrong classification.

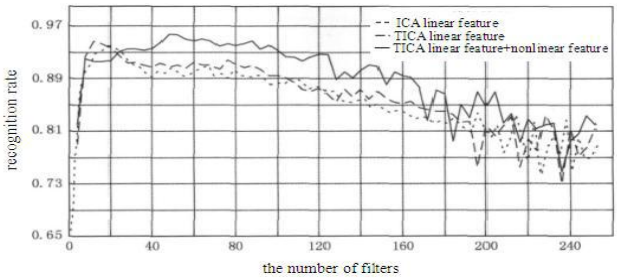

Figure 6. the recognition rate and the number of filters.

TABLE 1. THE TEST SAMPLE IDENTIFICATION RESULTS.

	0º belt fold over	Between 0º and 3thbelt butt open	0º Belt dispersion line	Belt layers along a direction	Foreign matter	Split belts	Belts open root	the number of correctly identified	The total number of samples	recognition correct rate %
0º belt fold over	39	0	1	0	0	0	0	39	40	97.50
Between 0º and 3thbelt butt open	0	49	0	0	0	1	0	49	50	98.00
0º Belt dispersion line	0	0	8	0	1	0	1	8	10	80.00
Belt layers along a direction	0	0	0	40	0	0	0	40	40	100.00
Foreign matter	0	0	2	0	68	0	0	68	70	97.14
Split belts	0	1	0	0	0	46	3	46	50	92.00
Belts open root	0	1	0	0	0	2	37	37	40	92.50
The total number of samples								287	300	93.88

All the rest defect types have very high recognition rates. This is because this paper estimates the basis functions and filters from the defect samples adaptation to the characteristics of defect images. Therefore, this feature extraction method is more effective than that by using generic transform. And the feature vector fully reflects the information of original images.

As to the time required for recognition, we only need to consider the time of sample feature extraction and the classification time of classifier, as filter only needs to be estimated once and off-line estimation. Simulation in Mat lab environment, for a 50 x 50 size of defect images uses the optimal number of filter to extract the 3 kinds of different features for recognition, and their recognition time were 11 m/s, 9m/s and 18m/s respectively. According to the actual situation of production line and experience, the proposed method can meet the requirements of real-time identification.

CONCLUSIONS

The conversion from the spatial domain to transform domain for defect images to extract their features can improve the recognition rate, but general linear transformation and the basis function are predefined and constant, and cannot adapt to the characteristics of defect image. Our basis functions filters are unsupervised learning and estimated adaptively based on ICA and TICA model from the tire defect library. the estimated basis in this paper has a stronger adaptability, and are suitable for the study of the characteristics of tire defect images. So it is more effective to extract the defect features than the general linear transform with the corresponding filter, and its overall recognition rate of defects can be up to 95.76%.

REFERENCES

1. T. Mäenpää, M. Impertinent and M. Pietikainen, “Real-Time Surface Inspection by Texture”,Real-Time Imaging., vol. 9, no. 5, 2003, pp. 289-296.
2. S.H. Chen and D.B. Perng, “Directional textures auto-inspection using principal component analysis”, Int J Adv Manuf Technol, 2011 55:1099–1110.
3. M. Sivalingamaiah and B.D. Venakramana Reddy, “Texture Segmentation Using Multichannel Gabor Filtering”, Journal of Electronics and Communication Engineering.,vol. 2, no. 6, 2012, pp. 22-26.
4. Z. Yan, L. Tao and L. Qingling, "Defect detection for tire laser shearography image using curve let transform based edge detector", Optics & Laser Technology., Vol. 47, 2013, pp. 64-71.
5. Z.D. Tsai and M.H. Perng, “Defect detection in periodic patterns using a multi-bandpass filter”, Machine Vision and Applications 2013, 24:551–565.
6. X. Yuanyuan, Z. Caiming and G. Qiang, “A Dictionary-based Method for Tire Defect Detecion”, Proceeding of the IEEE International Conference on Information and Automation Hailar, China, 2014, July 519-523.
7. M. Alper Selver, Vural Avşar & Hakan Özdemir, “Textural fabric defect detection using statistical texture transformations and gradient search”, The Journal of The Textile Institute., vol. 105, no. 9, 2014, pp. 998-1007.
8. W. Xiuyong, X. Ke and X. Jinwu, “Plate surface defect recognition method based on wavelet moment invariant and locality preserving projection”, Journal of University of Science and Technology Beijing., vol. 31, no. 10, (2009), pp. 1342-1346.
9. W. Xiuyong, X. Ke and X. Jinwu, “Automatic recognition method of surface defects based on Gabor wavelet and kernel locality preserving projection”, Acta Automatica Sinica., vol. 36, no. 3, 2010, pp.438-441.
10. A. Hyvärinen, P.O. Hoyer and M. Inki, “Independent Component Analysis”, Algorithms and Application., vol. 13, no. 4, 2000, pp. 411-430.
11. A. Hyvärinen, P.O. Hoyer and M. Inki, “Topographic Independent Component Analysis”, Algorithms and Application., vol. 13, no. 7, 2001, pp.1527-1558.
12. A. Hyvärinen, “Fast and Robust Fixed-Point Algorithms for Independent Component Analysis”, IEEE Transaction on Neural Networks., vol. 10, no. 3, 1999, pp. 626-634.